

## A RECTIFIED RESPONSE OF DAYTIME RADIO WAVE ABSORPTION TO SOUTHWARD AND NORTHWARD EXCURSIONS DURING NORTHWARD INTERPLANETARY MAGNETIC FIELD: A CASE STUDY

Masanori NISHINO<sup>1</sup>, Nozomu NISHITANI<sup>1</sup>, Natsuo SATO<sup>2</sup>,  
Hisao YAMAGISHI<sup>2</sup>, Mark LESTER<sup>3</sup> and Jan A. HOLTET<sup>4</sup>

<sup>1</sup>*Solar-Terrestrial Environment Laboratory, Nagoya University, Toyokawa 442-8507*

<sup>2</sup>*National Institute of Polar Research, Itabashi-ku, Tokyo 173-8515*

<sup>3</sup>*Department of Physics and Astronomy, University of Leicester, Leicester, LR1 7RH, U.K.*

<sup>4</sup>*Department of Physics, University of Oslo, Blindern, Oslo, Norway*

**Abstract:** An example of daytime radio wave absorption at 30 MHz observed by the Imaging Riometer at Ny-Ålesund (75.5° MLAT) is presented. Its characteristic feature is a type of slowly varying absorption (SVA) in the morning-noon sector during the northward interplanetary magnetic field (IMF). Furthermore a unique feature is that fluctuating variation superimposed upon the SVA showed a “rectified response” to alternate northward/southward IMF excursions, in particular, a pronounced response in the southern (low-latitude) part in the riometer field of view. From simultaneous *F*-region backscatter echoes observed by Finnish HF radar and electron fluxes by the DMSP-satellite it is concluded that the daytime absorption is likely caused by precipitation of eastward drifting auroral electrons generated by substorms in the midnight region. The rectified response is interpreted as follows: The boundary of the open-closed field line moves to the poleward/equatorward during the northward/southward IMF excursions, respectively, due to the magnetic reconnections at the low-latitude boundary layer (LLBL)/cleft, and associated field-aligned currents (FAC) are intensified during the both IMF excursions. The precipitation of auroral electrons carried by upward FAC produces the absorption in the low-latitude (~75° MLAT) of Ny-Ålesund.

### 1. Introduction

The dynamic features of the cusp/cleft auroras and their relationships to the solar wind plasma and the interplanetary magnetic field (IMF) conditions provide us information on solar wind-magnetosphere interactions in the dayside magnetosphere. Recently SANDHOLT *et al.* (1998a) classified dayside auroral forms and activities in the high-latitude ionosphere according to the IMF orientation, based on ground auroral observations at Ny-Ålesund, Svalbard (75.5° magnetic latitude (MLAT), *L*-value ~16). The overview of the result was illustrated schematically for different regimes of the IMF orientation, and they have revealed that the IMF clock angle ( $B_y/B_z$ ) is a good parameter to classify different dayside auroras.

On the other hand, the Riometer (Relative Ionospheric Opacity METER) instrument which measures radio wave absorption in the ionosphere is sensitive for detecting the excess ionization created in the *D*- and lower *E*-region by precipitating auroral

electrons with energies up to several tens of keV (*e.g.* PENMAN *et al.*, 1979). The conventional Riometer technique with single broad-beam was advanced by the development of the Imaging Riometer for Ionospheric Studies (IRIS) first deployed at South Pole (DETRICK and ROSENBERG, 1990), which operates at a frequency of 38.2 MHz with a two-dimensionally 49 narrow-beam antenna. The IRIS has enabled us to obtain small-scale features (about 20 km near the zenith) of the ionospheric absorption.

Using the IRIS data at Sondrestrom ( $73.7^\circ$  invariant latitude), STAUNING *et al.* (1995a) demonstrated a type of daytime absorption observed near the magnetic noon, which showed pulsating and impulsive features with rather weak intensity ( $< 0.5$  dB) during the southward IMF. The absorption was closely related to the values of the east-west component ( $B_y$ ) of the IMF, and has been interpreted as electron heating due to the *E*-region Hall-currents (DPY currents) by strong horizontal electric fields associated with convection enhancements. By the complementary measurements of the ionospheric convection observed by Sondrestrom incoherent scatter (IS) radar, CLAUER *et al.* (1995) revealed that the absorption enhancement was associated with a latitudinally narrow and longitudinally limited intensification of the westward convection and associated eastward Hall currents. Using the absorption data obtained by four IRIS instruments installed in the European arctic region, NISHINO *et al.* (1997) revealed that such cusp-latitude *E*-region absorption showed a poleward motion of front-like features extending over 700 km in longitude associated with strongly negative IMF- $B_y$  ( $B_z \sim 0$ ). These results indicate that daytime absorption as well as dayside aurora in high latitudes is closely related to the IMF orientation.

ROSENBERG *et al.* (1993) demonstrated another type of daytime absorption observed near the magnetic noon by the IRIS at South Pole ( $-74^\circ$  invariant latitude). By comparison with 630.0 nm optical emissions and backscatter echoes by Halley PACE HF radar (BAKER *et al.*, 1989), they have suggested that the absorption may be related to *F*-region plasma patches drifting poleward from the dayside oval into the polar cap. Polar patches were associated with significant enhancements of plasma density in disturbed *F*-region ionosphere under the southward IMF (RODGER *et al.*, 1995). However, the observed absorption value was greater than theoretical *F*-region absorption calculated by using plasma data measured simultaneously by incoherent scatter (IS) radar (WANG *et al.*, 1994; NISHINO *et al.*, 1998).

We present an example of daytime radio wave absorption observed in the magnetic morning-prenoon sector at Ny-Ålesund on February 28, 1996. Its characteristic feature is a type of slowly varying absorption (SVA) during the northward IMF. Furthermore, a unique feature is that the absorption shows a "rectified response" to alternate northward/southward IMF excursions during the northward IMF. We first discuss mechanisms of this characteristic absorption, in comparison with simultaneous HF radar data, particle data from the polar-orbiting Defense Meteorological Satellite Program (DMSP) satellite and the ground geomagnetic network data. Further we discuss the rectified response with regards to electrodynamics in the dayside magnetosphere.

## 2. Observations

The IRIS installed at Ny-Ålesund operates at 30 MHz since September, 1991. The IRIS antenna consists of two-dimensional 64 narrow-beams. The detailed technique and data handling were reported by NISHINO *et al.* (1993). The projection of 64-beams with a  $-3$  dB beam-width to the ionospheric plane at 90 km altitude is shown in Fig. 1. Upward and downward directions are approximately towards geomagnetic north and south, respectively. The 64-beams are assigned to labels of N1, N2,..., N8 for the north to the south, and labels of E1, E2,..., E8 for the east to the west.

Figure 2 shows the location of the IRIS at Ny-Ålesund on the map of the European arctic region. The illumination sector of the beam-10 radiated from the Finnish HF radar, the path of the DMSP F13 satellite with time and the Svalbard geomagnetic stations used in this study are illustrated. The Finnish HF radar of CUTLASS (Cooperative UK Twin Located Auroral Sounding System) operates at Hankasalmi, Finland. The radar has 16 narrow-beams ( $\sim 3.25^\circ$  beam-width) directing poleward, scanned in 2 min and a range resolution of 45 km (YEOMAN *et al.*, 1997). The particle instrument in the DMSP satellite includes an auroral particle sensor which measures precipitating auroral electrons and ions from 30 eV to 30 keV energy ranges (NEWELL and MENG, 1992). The geomagnetic data are obtained from the IMAGE (International Monitor for Auroral Geomagnetic Effects) magnetometer network in Svalbard and northern Scandinavia (LÜHR *et al.*, 1998).

The upper panel of Fig. 3 shows the north-south ( $B_z$ ) and east-west ( $B_y$ ) components of the IMF from IMP-8 satellite during 0500–0900 UT on February 28, 1996.

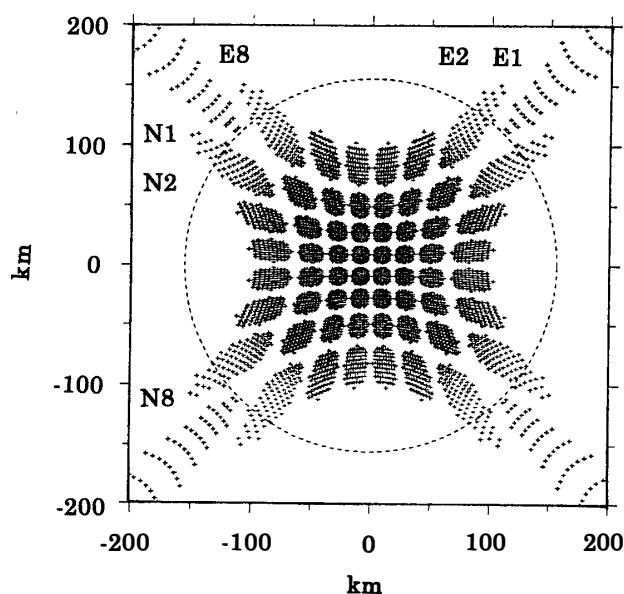


Fig. 1. The projection of the two-dimensional  $8 \times 8$  beams with a  $-3$  dB beam-width to the ionospheric plane at 90 km altitude. The beams are assigned to labels of N1, N2, ..., N8 for the geomagnetic north to the south, and E1, E2, ..., E8 for the geomagnetic east to the west.

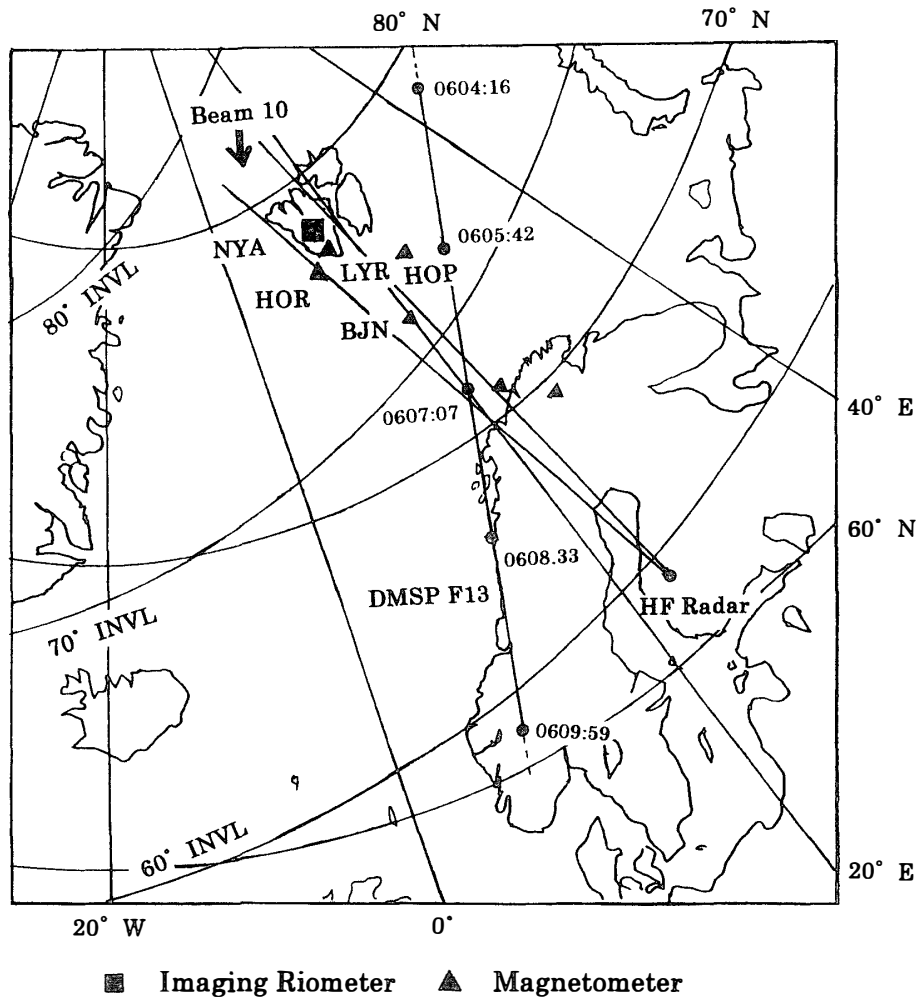


Fig. 2. The location of the imaging riometer installed at Ny-Ålesund. The illumination sector (solid lines) of the beam-10 radiated from the Finland HF radar, the footprints of the DMSP F13 path with time and the locations of the Svalbard geomagnetic stations in the IMAGE magnetometer network are displayed in the European arctic region.

The satellite was favorably located upstream beyond the dayside magnetopause ( $X \sim +34 R_E$ ,  $Y \sim -3 R_E$ ,  $Z \sim +20 R_E$  in GSE). The  $B_z$ -component changed from negative (southward) to positive (northward) at about 0530 UT, and remained positive until about 0730 UT with an abrupt southward excursion and an immediate northward return around 0620 UT. The  $B_z$ -component decreased gradually thereafter to near zero until about 0720 UT and changed eventually to negative. The  $B_y$ -component shows the repetition ( $\sim 30$  min) of negative and positive excursions during 0500–0720 UT. The  $B_x$ -component was always positive during the same time period.

The lower panel of Fig. 3 shows time variations in the ionospheric absorption during 0500–0900 UT at Ny-Ålesund. The variations are displayed in the north-south (N2–N8) and east-west (E2–E8) beam cross-sections centered at the specific beam N4 E7 (see Fig. 1). One division of the absorption value is 0.7 dB. The magnetic noon

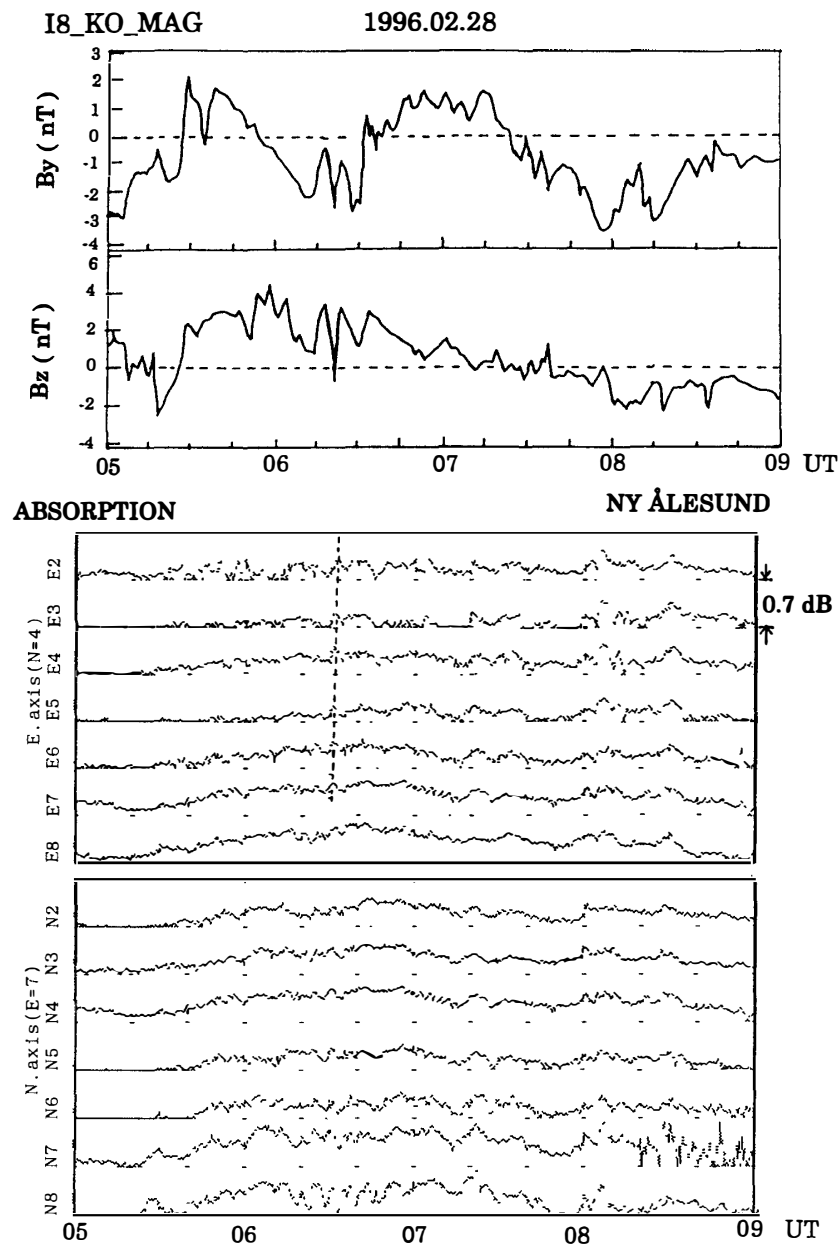


Fig. 3. Upper panel: Time variations in the east-west component ( $B_y$ ) and the north-south component ( $B_z$ ) of interplanetary magnetic field (IMF) from IMP-8 satellite during 0500–0900 UT on February 28, 1996. Lower panel: Time variations in the ionospheric absorption in the north-south and east-west cross-sections centered at the N4E7 beam observed by the imaging riometer at Ny-Ålesund. Absorption scale is 0.7 dB/div. The time-axis of the IMF-variation is shifted backward by 10 min to explain the relationship between the IMF and the absorption.

at Ny-Ålesund is approximately 0850 UT, so that the absorption during the northward IMF was observed there in the magnetic morning-noon sector.

It should be noted that the time-axis of the IMF variation is shifted backward by 10 min to compare the relationship between the IMF and the absorption variation, taking

account of the propagation delay from the IMP-satellite position to the polar ionosphere. STAUNING *et al.* (1995a) calculated the delay times for the following three segments, (a) from the IMP-satellite to the bow shock front, (b) the shock front to the magnetopause subsolar point, and (c) the magnetopause to the ionospheric footprint in the cusp region. They estimated total 7.5 min delay for the IMP-8 position of  $X \sim +19.2$  Re in GSE assuming solar wind velocity of 500 km/s. By the same estimation for the  $X \sim +34$  Re described above we obtain 10.6 min delay. Practically we estimate the delay time by analyzing a cross-correlation with 1 min time-difference between the  $B_z$ -component and the absorption (E7N8) variation in the time period (0540–0615 UT) of the positive IMF. The obtained cross-correlation represents a peak coefficient ( $\sim 0.75$ ) by 10 min delay, which indicates a reasonable delay time between them. The high correlation is also obtained for the zenith beam. In the following discussion, different UT is used between the IMF and the absorption.

The absorption increased slowly in all channels around 0540 UT ( $\sim 0850$  MLT), associated with a gradual northward change of the  $B_z$ -component at 0528 UT, and reached a maximum value ( $\sim 0.6$  dB at the E7N8 beam) at 0612 UT, corresponding to the peak ( $\sim +4$  nT) of the  $B_z$ -component near 0600 UT. This absorption intensity equals to about 0.4 dB for the vertical absorption. Subsequently the  $B_z$ -component showed southward/northward excursions; the  $B_z$ -component first decreased to about  $+1$  nT until 0613 UT, and increased immediately to  $+3.8$  nT at 0616 UT, followed by an abrupt southward excursion reaching  $-0.5$  nT with an immediate northward return to  $+3.7$  nT at 0620 UT, and thereafter decreased to about  $+1$  nT until 0630 UT, and increased to about  $+3$  nT until 0635 UT. The  $B_y$ -component showed positive during 0530–0555 UT, negative during 0555–0632 UT including abrupt positive and negative excursions, and again positive during 0632–0725 UT. Corresponding to the northward/southward excursions, the absorption showed a characteristic fluctuation in the all channels during 0615–0650 UT, particularly, a pronounced fluctuation with greater amplitude at the west-southernmost beam (E7N8). It is remarked from the east-west beam cross-section that the absorption showed eastward motion ( $\sim 1.3$  km/s) near 0630 UT, as displayed by a dashed line (excluding the E8-beam for ambiguity due to the grating-beam), associated with the abrupt southward excursion. Thereafter the absorption showed a gradual time-variation until about 0740 UT. In the following, we examine in detail the relationship between the absorption and the IMF, focusing on the fluctuating absorption in the time period of 0610–0650 UT.

The upper panel of Fig. 4 shows a time variation of the clock angle ( $\theta = \arctan(B_y/B_z)$ ) of the IMF-B defined by the  $B_y$ - and  $B_z$ -components. Positive angles represent clockwise ones measured from the north IMF. The lower panel shows the absorption variation at the specific E7N8 beam. Here we notice a peculiar feature in the fluctuating absorption during the time period; the absorption increases marked with small circles correspond to the northward excursions, and the absorption increases with small triangles correspond to the southward excursions. This feature indicates a “rectifying response” of the absorption to alternate southward/northward IMF excursions. The crossover of the response is appropriately determined by  $\theta \doteq -45^\circ$  (in the northward/dawnward plane of the IMF) in the clock angle, as indicated by a dotted line.

The geomagnetic activity varied rather high to moderate conditions: Three-hour  $K_p$

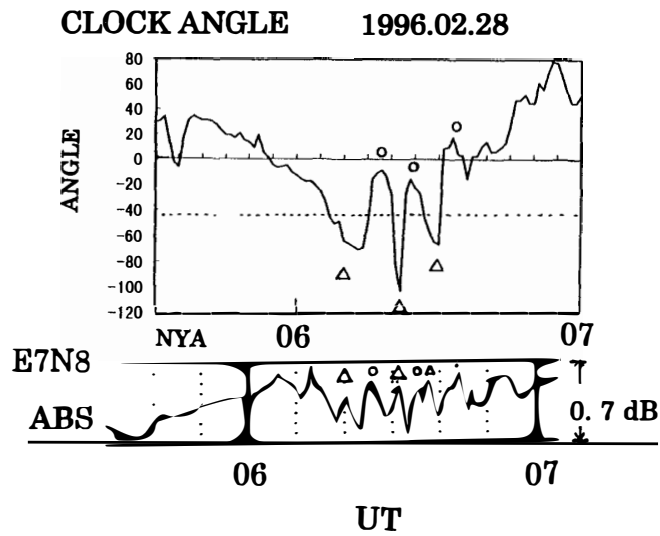


Fig. 4. Upper panel: Time variation in the clock angle ( $\theta = \arctan (B_y/B_z)$ ) of the IMF-B defined by  $B_y$ - and  $B_z$ -components. The time-axis of the IMF clock angle is shifted backward by 10 min. Lower panel: Time variation in the absorption at the specific E7N8 beam.

IMAGE magnetometer network 27-28 FEB 1996

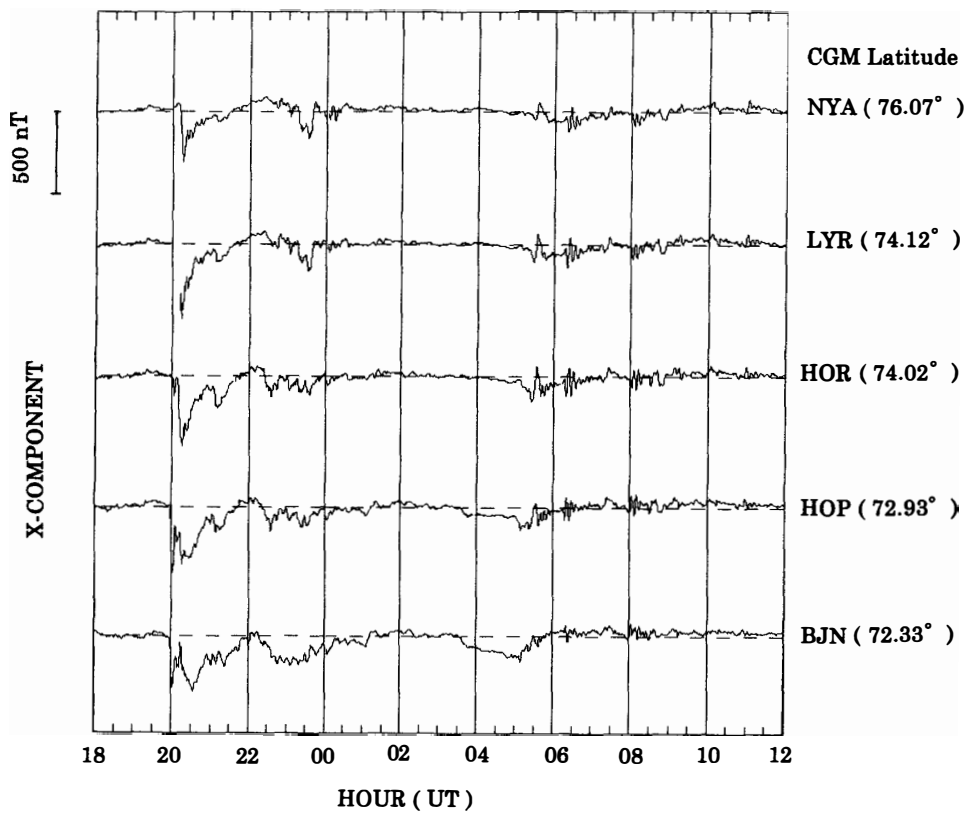


Fig. 5. Time variations in the geomagnetic X-components at Svalbard stations in the IMAGE magnetometer network. The name and the geomagnetic latitude of the stations are noted at the right side.

indices were 4 and 4- for 18 h–21 h and 21 h–24 h UT on February 27, and 3, 4- and 2- for 0 h–3 h, 3 h–6 h and 6 h–9 h UT on February 28, respectively. Figure 5 shows time variations of the geomagnetic  $X$ -components at Svalbard stations in the IMAGE magnetometer network (see Fig. 2). The name and the corrected geomagnetic latitudes of the stations are marked on the right side of the geomagnetic data (LÜHR *et al.*, 1998). The geomagnetic  $X$ -component at Ny-Ålesund recorded a sharp decrease ( $\sim -350$  nT at maximum) near 2010 UT on February 27, associated with substorm activity, and recovered at 22 h UT. Thereafter the  $X$ -component showed a negative bay ( $\sim -170$  nT at maximum) around 2330 UT. Geomagnetic positive deflections around 0530 UT and pulsating variations during about 0620–0650 UT showed a poleward progression with the velocity of about 1.5 km/s among the Svalbard stations.

### 3. Discussion

First we discuss mechanisms of the absorption observed in the morning-prenoon sector during the northward IMF. The high-latitude ionosphere is generally quiet under the northward IMF condition. RUOHONIEMI *et al.* (1993) examined the response of the high-latitude dayside ionosphere in the magnetic prenoon interval to an abrupt northward IMF transition from Goose Bay HF radar observations. They exhibited that backscatter echoes showed a dramatic decrease on the northward IMF transition, and also a disappearance of  $F$ -region structure on the meridional electron density profile which existed before the northward IMF transition. Therefore we examined backscatter echoes observed simultaneously by the Finnish HF radar.

Figure 6 displays range-time diagrams of the three parameters (velocity, echo power and spectral width) of backscatter echoes during 0600–1000 UT measured by the beam-10 of the HF radar (see Fig. 2). The values of the velocity (m/s), echo power (dB) and spectral width (m/s) are displayed by color codes on the right side of the respective diagram. Plus and minus signs of the velocity represent flow motions toward and away from the radar site, respectively. The ground distance from the Finnish radar site to Ny-Ålesund is about 2100 km, which is indicated by a thin horizontal broken line in the upper panel.

The echo power was enhanced at 0630 UT in the higher-latitude ( $78$ – $79^\circ$  MLAT) region north of Ny-Ålesund and persisted until about 0800 UT. However, as shown in Fig. 3, the morning absorption already increased at about 0530 UT when the  $B_z$ -component turned gradually from southward to northward. In addition, strong echoes displayed by a red color are seen at about 2500 km distance at about 0650 UT and 0715 UT. However, the absorption showed no specific enhancement at these corresponding times. These results indicate that the morning-prenoon absorption relates unlikely to a dynamic structure of the electron density in the  $F$ -region irregularities.

As we mentioned at the introduction, STAUNING *et al.* (1995a) demonstrated the cusp-latitude  $E$ -region absorption near the magnetic noon which was due to electron heating by strong ionospheric electric fields associated with the convection enhancement during the southward IMF. The motion of scattering irregularities in the high-latitude  $F$ -region observed by the HF-radar is known to be dominated by the convection drift of the ambient plasma (VILLAIN *et al.*, 1985; RUOHONIEMI *et al.*, 1987). As is seen from the



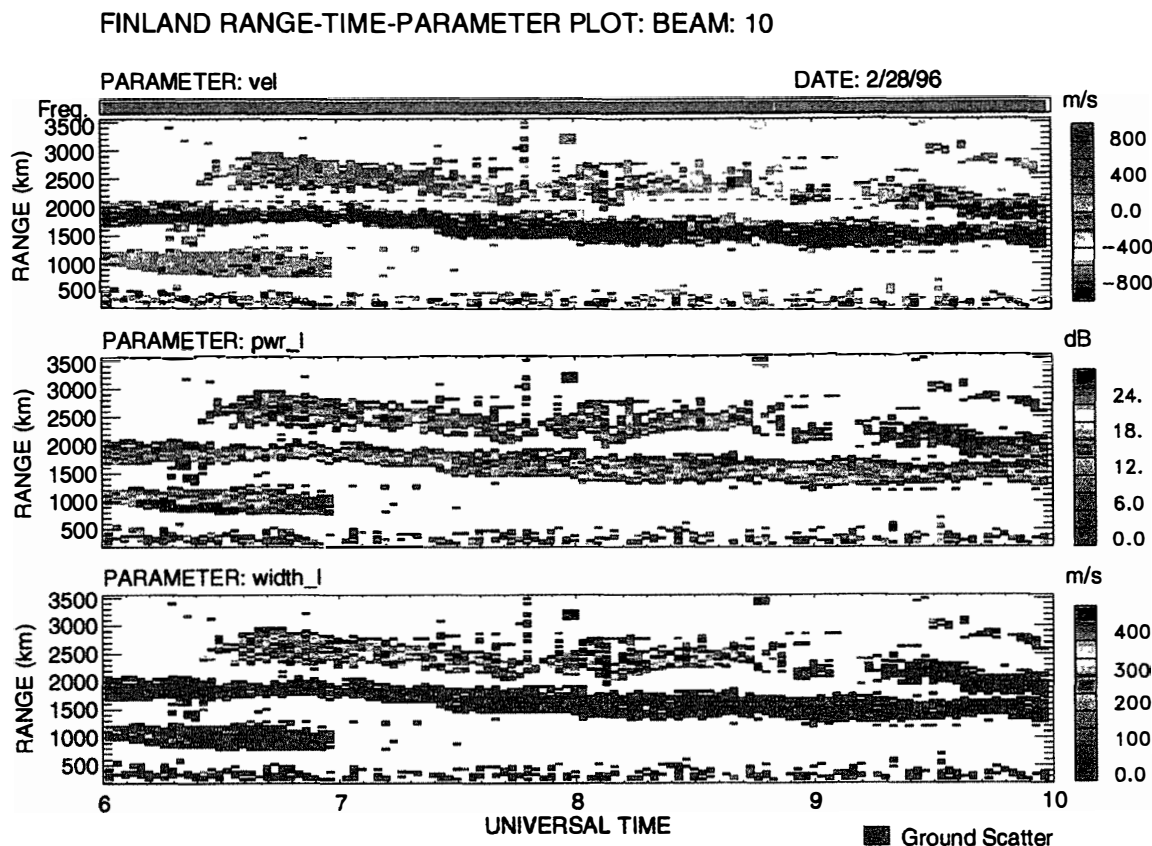


Fig. 6. Three diagrams showing range-time-parameter plot of velocity (m/s), echo power (dB) and spectral width (m/s) of backscatter echoes obtained by the beam-10 of the Finnish HF radar. The values of the parameters are displayed by color codes. Plus and minus signs of the velocity represent the flow toward and away from the radar site, respectively. A broken line in the velocity plot shows the 2100 km distance from the radar site.

velocity diagram in Fig. 6, the  $F$ -region convection drift was enhanced at 0630 UT when the  $B_z$ -component showed an abrupt southward excursion (0620 UT in the IMF-time). Around 0650 UT during the northward IMF, the line-of-site drift velocity attained at about 600 m/s toward the HF radar site, which velocity would induce electric field of 32 mV/m in the polar ionosphere. If this electric field extends to the  $E$ -region near Ny-Ålesund, the increase of electron temperature caused by the electric field through the two-stream instability (SCHLEGEL and ST-MAURICE, 1981), that is, the increase of electron-neutral collision frequency would be small, because the induced electric field is slightly beyond the threshold ( $\sim 25$  mV/m) (MEHTA and D'ANGELO, 1980). This fact predicts too small absorption ( $< 0.1$  dB) due to the  $E$ -region electron heating (STAUNING, 1995). Consequently the present absorption during the northward IMF is not attributable to the both mechanisms of  $E$ -region electron heating and  $F$ -region irregularities.

STAUNING (1996) demonstrated the slowly varying absorption (SVA) in the morning sector from the IRIS observations at Sondre Stromfjord ( $73.5^\circ$  MLAT), and has revealed that the SVA event is most likely a result from some drizzle precipitation of the eastward drifting auroral electrons (30–300 keV) generated by substorm activity in the

midnight region. In some cases, the SVA events exhibited strong pulsating with periods in the  $Pc$  4–5 range (STAUNING *et al.*, 1995b). The present absorption beginning at about 0530 UT ( $\sim$ 0840 MLT) evidently demonstrate the SVA feature without impulsive enhancements. As shown in Fig. 5, the geomagnetic  $X$ -components in Svalbard recorded a sharp decrease near the midnight ( $\sim$ 20 h UT) on the previous day associated with substorm. If the morning absorption is originated from this substorm, the time difference between them becomes unreasonably about 10 hours. Therefore we examine geomagnetic and riometer data obtained from CANOPUS (Canadian Auroral Network for OPEN Unified Study) ground-based network which was situated in the midnight sector around 6 h UT. We have found strongly enhanced electrojet currents (250–300 nT) and auroral absorption near 0445 UT on February 28 associated with substorm (by courtesy of G. ROSTOKER). About 45 min delay of the morning absorption ( $\sim$ 0530 UT) from the substorm onset is reasonable time in comparison with developing time at  $L = 14$  on global eastward movement of an auroral absorption event which is initiated on the midnight meridian near the region of maximum absorption (HARGREAVES, 1968). Thus it is evident that the present SVA is caused by precipitation of the eastward drifting auroral electrons generated by substorm activity in the midnight.

Here we investigate particle data from DMSP F-13 satellite (nearly circular polar orbit at about 800 km altitude) during the present absorption event in order to have information on electron precipitation. The satellite passed through from the eastern region of Svalbard to the northern Scandinavia during 0604–0610 UT (see Fig. 2). Figure 7 shows spectrograms of electron and ion fluxes versus energy and time, in which the particle regimes inferred from the satellite particle data are marked beneath the axis (NEWELL and MENG, 1992). Note that the ion energy scale is inverted. Color scales represent differential energy fluxes in log-scale. At about 0604 UT, the satellite was located from Ny-Ålesund by about  $30^\circ$  in longitude along the same invariant latitude, corresponding to the boundary plasma sheet (BPS) in the magnetosphere. Precipitating electrons were ranged from 0.1 keV to near 30 keV energies with spectrally and spatially sporadic electrons, which structure is very similar to the spectrogram during the northward IMF provided by NEWELL *et al.* (1991). At about 0605 UT when the satellite approached most closely to the southern region ( $73^\circ$  MLAT) of Ny-Ålesund, the energy range extended over 30 keV, indicating that precipitation of energetic electrons from the central plasma sheet (CPS) contributed to  $D$ - or lower  $E$ -region absorption. The characteristics of these particle data are consistent with the statistical result that  $\sim$ 9 h MLT sector at the Ny-Ålesund latitude corresponds to the transition region from traditional CPS to BPS (NEWELL and MENG, 1992).

SANDHOLT *et al.* (1993) revealed that the cleft aurora with green line emissions of 1–15 kR during the southward IMF was caused by electron precipitation from the low-latitude boundary layer (LLBL)/BPS by utilizing particle data within  $71$ – $72^\circ$  MLAT from the DMSP satellite. The cleft aurora at Ny-Ålesund showed strong green line emissions (several kR) near 0600 UT during the northward IMF, which covered most of the field of view ( $74^\circ$ – $78^\circ$  MLAT) of the meridian scanning photometer (SANDHOLT *et al.*, 1998a). Plasma sources of the cleft aurora were thought to be a mixture of LLBL and BPS. They classified the cleft aurora as the type 4 aurora appearing in the morning-prenoon sector which had wide variability in time and

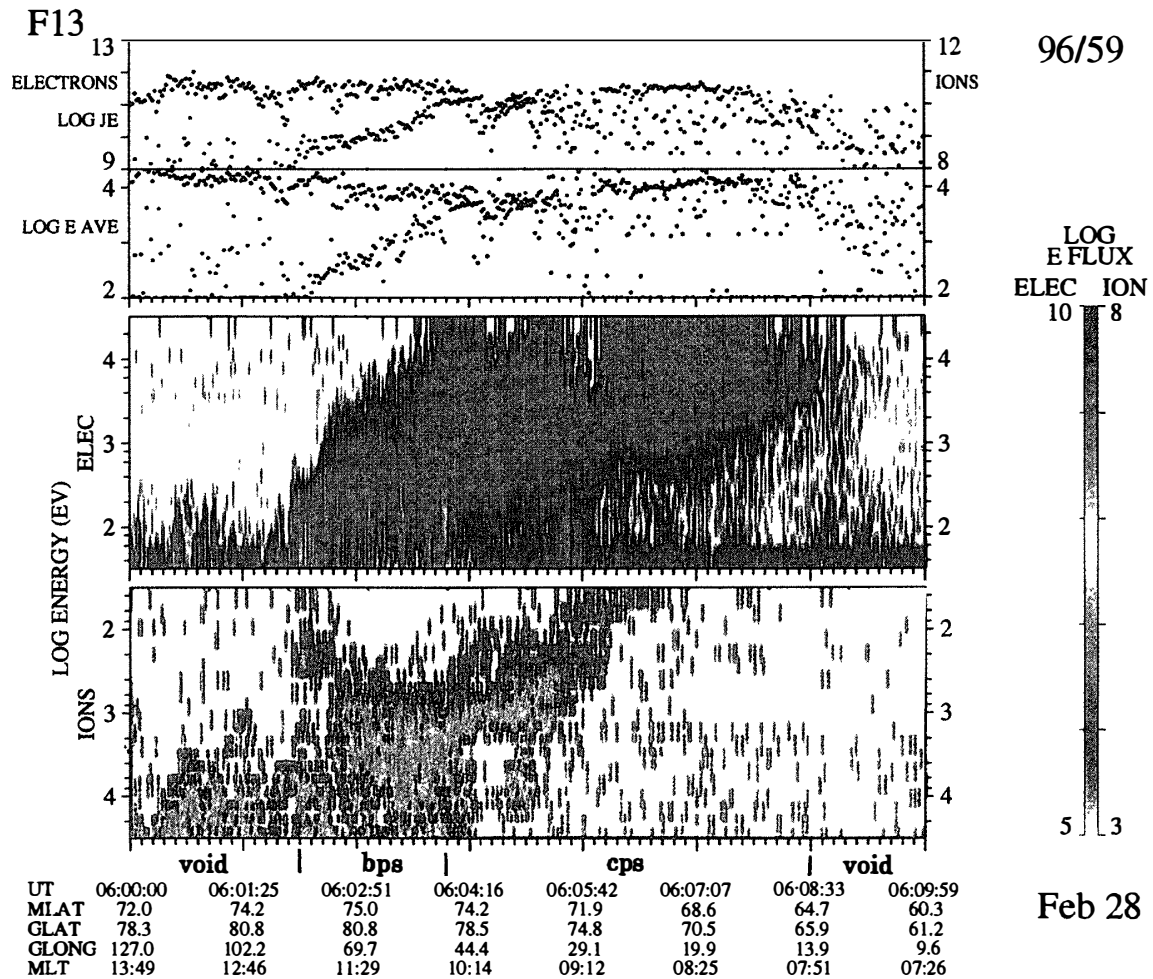


Fig. 7. Differential energy spectrograms of electron and ion fluxes from the DMSP F13-satellite during 0600–0610 UT on February 28, 1996. The particle regimes are marked beneath the axis (NEWELL and MENG, 1992). Color scales represent differential energy flux in log scale. The top panel shows the electron and ion integral energy fluxes and average energy.

exhibited an east-west inhomogeneity in the lower latitude region ( $\sim 75^\circ$  MLAT). The characteristics of this cleft aurora indicate that the present morning-noon absorption is probably connected to the auroral electrons in the LLBL/BPS which drifted eastward from the nightside BPS/CPS.

In the following we concentrate on the discussion of the “rectified response” discovered in the fluctuating absorption. The response is represented as the crossover angle of  $-45^\circ$  (northward/dawnward) in the IMF clock angle. This crossover angle is thought to be reasonable from the anti-parallel field condition of the geomagnetic field line configuration in the cleft. SANDHOLT (1991) demonstrated discrete auroras at the poleward boundary of the cusp/cleft aurora within 1030–1230 MLT at Ny-Ålesund during the northward IMF, and inferred a balanced pair of upward and downward field aligned currents (FAC) within  $75^\circ$ – $77^\circ$  MLAT from the simultaneous DMSP F-7 satellite observation. He has also inferred that FAC/plasma flow indicate a generator

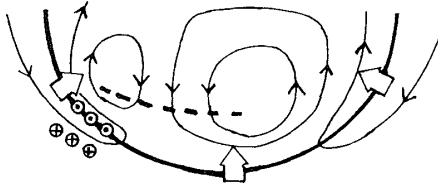
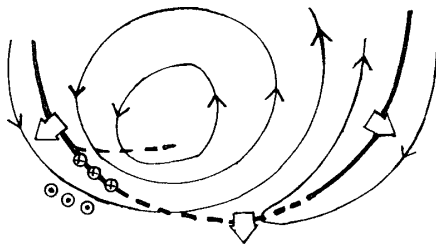
(a) IMF  $B_z > 0$ ,  $B_y < 0$ (b) IMF  $B_z \sim 0$ ,  $B_y < 0$ 

Fig. 8. Two sketches of the dayside convection flow pattern and field aligned current (FAC) for  $B_z > 0$  and  $B_z \sim 0$  during  $B_y < 0$ . Upward and downward FAC are represented by circles with dot and cross marks, respectively. Bold solid-lines represent adiabatic segments of the open-closed field line boundary, arrow solid-lines are streamlines, bold dashed-lines are the ionospheric images of the magnetopause reconnection regions. The open arrows indicate the motions of the open-closed field line boundary (modified from SANDHOLT *et al.*, 1998b).

mechanism poleward the cusp/cleft during the northward IMF. From these inferences, SANDHOLT *et al.* (1998b) illustrated three basic configurations of the dayside plasma flow and cusp precipitation in the northern hemisphere on the IMF conditions of the southward ( $B_z < 0$ ), northward ( $B_z > 0$ ) and near zero ( $B_z \sim 0$ ) during the negative  $B_y$ .

In Fig. 8, we show two configurations of the dayside plasma flow pattern and FAC on the IMF conditions of  $B_z > 0$  and  $B_z \sim 0$  during  $B_y < 0$ , modified from SANDHOLT *et al.* (1998b), where bold solid lines represent adiabatic segments of the open-closed field line boundary, arrow solid-lines are streamlines and bold dashed lines are the ionospheric images of the magnetopause reconnection regions. During  $B_z > 0$  (a), the magnetic reconnection occurs at the higher-latitude magnetopause (e.g. BASINSKA *et al.*, 1992) and their ionospheric images would be located at  $\sim 78^\circ$  MLAT. This may be evidenced from the statistical result that the cusp shows a feature of the widely spread spectral-width in the high-latitude HF radar echoes (see Fig. 6) (LESTER, 1998), and also is sustained from the auroral observations that the dayside cusp auroras are located at the poleward boundary of  $\sim 78^\circ$ – $79^\circ$  MLAT during the northward IMF (SANDHOLT *et al.*, 1998a, b). Associated with the magnetic reconnection at the magnetopause, the FAC would be intensified, showing upward FAC at the poleward open-closed field line boundary ( $\sim 75^\circ$  MLAT) and downward FAC in the vicinity of the convection reversal in the prenoon. Subsequently, associated with the rotation of the IMF clock angle toward  $B_z \sim 0$  (b), the reconnection region, thus the field line boundary would move equatorward with convection enhancement in the prenoon sector. This may be evidenced from the equatorward drift motion of the *F*-region irregularities (see Fig. 6). The eastward motion of the absorption seen near 0630 UT (see Fig. 3) also may manifest the enhanced eastward (sunward) convection in the prenoon sector. The associated FAC would be also intensified, showing upward FAC at the equatorward boundary ( $75^\circ$  MLAT) and downward FAC at the poleward boundary. Consequently, accompanied with the alternate northward/southward IMF excursions, the open-closed

field line boundary moves to poleward/equatorward, respectively, in the prenoon on the  $B_y < 0$  condition. The associated FAC are intensified on the both conditions of the IMF excursions, and thus the precipitation of downward streaming electrons carried by the upward FAC at the LLBL/cleft produces the fluctuating absorption with the “rectified response” at the low latitude ( $\sim 75^\circ$  MLAT) of Ny-Ålesund.

## 5. Conclusion

The daytime radio wave absorption was observed in the magnetic morning-prenoon sector during the northward IMF by the imaging riometer at Ny-Ålesund. The *F*-region backscatter echoes observed simultaneously by Finnish HF radar were located at the higher-latitude than Ny-Ålesund, indicating no absorption associated with strong *F*-region irregularities. Also the drift velocity of the convection during the northward IMF induced a small ionospheric electric field, indicating no absorption due to the *E*-region electron heating. Thus it is concluded that the present absorption showing the feature of the SVA is caused by the precipitation of eastward drifting auroral electrons in the BPS/CPS generated by substorm activity. This conclusion is supported by the detection of energy spectra ( $\sim 30$  keV) of electron fluxes from the DMSP-F13 satellite passing through the same magnetic latitude with Ny-Ålesund in this time period. The “rectified response” of the prenoon absorption is interpreted that the convection boundary moved poleward/equatorward associated with the alternate northward/southward IMF excursions, respectively. The associated FAC were intensified with the both IMF excursions, and the precipitation of down streaming auroral electrons carried by the upward FAC produced the absorption at the low latitude of Ny-Ålesund.

This case study suggests a significant indication that the morning-prenoon absorption is an ionospheric signature of the magnetic reconnection at the LLBL/cleft at the magnetopause. Further analysis of the IRIS data are needed to understand the LLBL/cleft absorption feature in relation to the IMF orientation and its transient variation. Studies of the ionospheric absorption by geomagnetic conjugate IRIS observations between the northern and southern polar hemispheres will provide more useful information for understanding of solar wind-magnetosphere interactions in the dayside magnetosphere.

## Acknowledgments

We would like to thank A. EGELAND, University of Oslo, for arranging the riometer observations at Ny-Ålesund, and T. OGAWA, Nagoya University, for helpful comments. We gratefully acknowledge Ron LEPPING, NASA Goddard Flight Center, for the IMP 8 IMF data, and also P. T. NEWELL and C. I. MENG, John Hopkins University, for the DMSP particle data. The geomagnetic data were provided from IMAGE magnetometer network through the web services. We also kindly acknowledge K. MAKITA, Takushoku University, for his help of analyzing DMSP data.

## References

- BAKER, K.B., GREENWALD, R.A., RUOHONIEMI, J.M., DUDENEY, J.R., PINNOCK, M., MATTIN N. and LEONARD J.M. (1989): Polar Anglo-American conjugate experiment. *EOS: Trans.*, **70**, 785, 799.
- BASINSKA, E.M., BUKKE, W.J., MAYNARD, N.C., HUGHES, W.J., WINNIGHAM, J.D. and HANDSON, W.B. (1992): Small-scale electrodynamic of the cusp with northward interplanetary magnetic field. *J. Geophys. Res.*, **97**, 6369–6379
- CLAUER, C.R., STAUNING, P., ROSENBERG, T.J., FRIIS-CHRISTENSEN, E., MILLER, P.M. and SITAR, R. (1995): Observations of a solar-wind-driven modulation of the dayside ionospheric DPY current system. *J. Geophys. Res.*, **100**, 7697–7713.
- DETRICK, D.L. and ROSENBERG, T.J. (1990). A phased-array radio wave imager for studies of cosmic noise absorption. *Radio Sci.*, **25**, 325–338.
- HARGREAVES, J.K. (1968): Auroral motions observed with riometers: Latitudinal movements and a meridian global pattern. *J. Atmos. Terr. Phys.*, **30**, 1463–1470.
- LESTER, M. (1998): Coherent-scatter radar studies of the dayside cusp. *Polar Cap Boundary Phenomena*, ed. by J. MOEN *et al.* Kluwer Academic Publ., 219–232 (NATO ASI series, series C, Vol. 509).
- LUHR, H., AYLWARD, A., BUCHER, S.C., PAJUNPAA, A., PAJUNPAA, K., HOLMBOE, T. and ZALEWSKI, S.M. (1998): Westward moving dynamic substorm features observed with the IMAGE magnetometer network and other ground-based instruments. *Ann. Geophys.*, **16**, 425–440.
- MEHTA, N. and D'ANGELO, N. (1980): Cosmic noise 'Absorption' by *E* region plasma waves. *J. Geophys. Res.*, **85**, 1779–1782.
- NEWELL, P.T. and MENG, C.I. (1992): Mapping the dayside ionosphere to the magnetosphere according to particle precipitation characteristics. *Geophys. Res. Lett.*, **19**, 609–612.
- NEWELL, P.T., WILLIAM, J.B., ENNIO, R.S., MENG, C -I., GREENSPAN, M.E. and CLAUER, C.R. (1991): The low-latitude boundary layer and the boundary plasma sheet at low altitude: Prenoon precipitation regions and convection reversal boundaries. *J. Geophys. Res.*, **96**, 21013–21023.
- NISHINO, M., TANAKA, Y., OGUTI, T., YAMAGISHI, H. and HOLTET, J.A. (1993): Initial observation results with imaging riometer at Ny-Ålesund ( $L=16$ ). *Proc. NIPR Symp. Upper Atmos. Phys.*, **6**, 47–61.
- NISHINO, M., YAMAGISHI, H., STAUNING, P., ROSENBERG, T.J. and HOLTET, J.A. (1997): Location, spatial scale and motion of radio wave absorption in the cusp-latitude ionosphere observed by imaging riometers. *J. Atmos. Solar-Terr. Phys.*, **59**, 903–924.
- NISHINO, M., NOZAWA, S. and HOLTET, J.A. (1998): Daytime ionospheric absorption features in the polar cap associated with poleward drifting *F*-region plasma patches. *Earth Planets Space*, **50**, 107–117.
- PENMAN, J.M., HARGREAVES, J.K., and MCLLWAIN, C.E. (1979): The relation between 10 to 80 keV electron precipitation observed at geosynchronous orbit and auroral radio absorption observed with riometers. *Planet. Space Sci.*, **27**, 445–451.
- RODGER, A.S., MENDE, S.B., ROSENBERG, T.J. and BAKER, K.B. (1995): Simultaneous optical and HF radar observations of the ionospheric cusp. *Geophys. Res. Lett.*, **22**, 2045–2048.
- ROSENBERG, T.J., WANG, Z., RODGER, A.S., DUDENEY, J.R. and BAKER, K.B. (1993): Imaging riometer and HF radar measurements of drifting *F* region electron density structures in the polar cap. *J. Geophys. Res.*, **98**, 7757–7764.
- RUOHONIEMI, J.M., GREENWALD, R.A., BAKER, K.B. and VILLAIN, J.P. (1987): Drift motion of small scale irregularities in the high latitude *F*-region. *J. Geophys. Res.*, **92**, 4553.
- RUOHONIEMI, J.M., GREENWALD, R.A., BEAUJARDIÈRE, DE LA, O. and LESTER, M. (1993): The response of the high-latitude dayside ionosphere to an abrupt northward transition in the IMF. *Ann. Geophys.*, **11**, 544–555.
- SANDHOLT, P.E. (1991): Auroral electrodynamic at the cusp/cleft poleward boundary during northward interplanetary magnetic field. *Geophys. Res. Lett.*, **18**, 805–808.
- SANDHOLT, P.E., FARRUGIA, C.L., MOEN, J., NORRABERG, O., LYBEKK, B., STEN, T. and HANSEN T. (1998a): A classification of dayside auroral forms and activities as a function of interplanetary magnetic field orientation. *J. Geophys. Res.*, **103**, 23325–23345.
- SANDHOLT, P.E., FARRUGIA, C.J., MOEN, J. and COWLEY, S.W.H. (1998b): Dayside auroral configurations: Response to southward and northward rotations of the interplanetary magnetic field. *J. Geophys.*

- Res., **103**, 20279–20295.
- SANDHOLT, P.E., MOEN, J., RUDLAND, A., OPSVIK, D., DENIG W.F. and HANSEN, T. (1993): Auroral event sequences at the dayside polar cap boundary for positive and negative interplanetary magnetic field  $B_y$ . J. Geophys. Res., **98**, 7737–7755.
- SCHLEGEL, K. and ST-MAURICE, J.P. (1981): Anomalous heating of the polar  $E$  region by unstable plasma waves, 1. Observations. J. Geophys. Res., **86**, 1447–1452.
- STAUNING, P. (1995): Progressing IMF- $B_y$ -related polar ionospheric convection disturbances. J. Geomagn. Geoelectr., **47**, 735–758.
- STAUNING, P. (1996): Investigations of ionospheric radio wave absorption processes using imaging riometer techniques. J. Atmos. Terr. Phys., **58**, 753–764.
- STAUNING, P., CLAUER, C.R., ROSENBERG, T.J., FRIIS-CHRISTENSEN, E. and SITAR, R. (1995a): Observations of solar-wind-driven propagation of interplanetary magnetic field  $B_y$ -related dayside ionospheric disturbances. J. Geophys. Res., **100**, 7567–7585.
- STAUNING, P., YAMAGISHI, H., NISHINO, M. and ROSENBERG T.J. (1995b): Dynamics of cusp-latitude absorption events observed by imaging riometer. J. Geomagn. Geoelectr., **47**, 823–845.
- VILLAIN, J.P., CAUDAL, G. and HANUISE, C. (1985): A SAFARI-EISCAT comparison between the velocity of  $F$  region small-scale irregularities and the ion drift. J. Geophys. Res., **90**, 8433–8443.
- WANG, Z., ROSENBERG, T.J., STAUNING, P., BASU, P.S. and CROWLEY, G. (1994): Calculations of riometer absorption associated with  $F$ -region plasma structures based on Sondre Stromfjord incoherent scatter radar observations. Radio Sci., **29**, 209–215.
- YEOMAN, T.K., LESTER, M., COWLEY, S.W.H., MILAN, S.E., MOEN, J. and SANDHOLT, P.E. (1997): Simultaneous observations of the cusp in optical, DMSP and HF radar data. Geophys. Res. Lett., **24**, 2251–2254.

*(Received December 9, 1998; Revised manuscript accepted April 26, 1999)*